Check for updates

Research Communication

Biophysical Characterization of Alpers Encephalopathy Associated Mutants of Human Mitochondrial Phenylalanyl-tRNA Synthetase

Shruti Chakraborty[1]
Michael Ibba[2]
Rajat Banerjee[1]*

[1]Department of Biotechnology and Dr. B. C. Guha Centre for Genetic Engineering and Biotechnology, University of Calcutta, Kolkata, India
[2]Department of Microbiology, The Ohio State University, Columbus, Ohio

Abstract

Mutations in nucleus-encoded mitochondrial aminoacyl-tRNA synthetases (mitaaRSs) lead to defects in mitochondrial translation affecting the expression and function of 13 subunits of the respiratory chain complex leading to diverse pathological conditions. Mutations in the FARS2 gene encoding human mitochondrial phenylalanyl-tRNA synthetase (*Hs*mitPheRS) have been found to be associated with two different clinical representations, infantile Alpers encephalopathy and spastic paraplegia. Here we have studied three pathogenic mutants (Tyr144Cys, Ile329Thr, and Asp391Val) associated with Alpers encephalopathy to understand how these variants affect the biophysical properties of the enzyme. These mutants have already been reported to have reduced aminoacylation activity. Our study established that the mutants are significantly more thermolabile compared to the wild-type enzyme with reduced solubility in vitro. The presence of aggregation-prone insoluble *Hs*mitPheRS variants could have a detrimental impact on organellar translation, and potentially impact normal mitochondrial function. © 2019 IUBMB Life, 71(8): 1141–1149, 2019

Keywords: *Hs*mitPheRS; infantile Alpers encephalopathy; mitaaRSs

INTRODUCTION

Mitochondria are known as the power house of cell because they are the major source of ATP synthesis through aerobic respiration involving the respiratory chain (RC) complexes located in the mitochondrial membrane. Defects in the fundamental functions of RC complexes have been linked to a growing list of human disorders including mitochondrial myopathy, encephalopathy, lactic acidosis, and stroke-like episodes (MELAS), myoclonic epilepsy with ragged red fibers (MERRF), diabetes and deafness (1–3). Mitochondria maintain a separate genome and the human mitochondrial genome encodes 13 subunits of RC complexes, 2 rRNAs, and 22 tRNAs (4). Most of the mitochondrial translational machinery is encoded by the nuclear genome and transported into mitochondria including tRNA modifying enzymes, translation elongation and termination factors and mitaaRSs. Mutations in maternally inherited mitochondrial DNA have been found to be associated with many of the mitochondrial diseases and the most commonly reported class of pathogenic mutations have been reported in tRNA encoding genes (5–8). However, it was found that the aminoacylation of mitochondrial tRNAs may also be impaired due to mutations in nuclear-encoded mitaaRSs and an expanding list of mutations in mitaaRSs encoding genes have been reported to be associated with mitochondrial disorders (9). Though functional mitochondria are very much essential for every cell, defects in mitochondrial translation due to reduced mitaaRS activity have been found to be highly tissue-specific in patients. The affected mitaaRS is often identifiable from the symptoms alone as the pattern of the

Abbreviations: *ANS, 8-Anilino-1-naphthalenesulfonic acid; d_H, hydrodynamic diameter; DLS, Dynamic light scattering;* Hs*mitPheRS, human mitochondrial phenylalanyl-tRNA synthetase; LBSL, leukoencephalopathy with brain stem and spinal cord involvement and lactate elevation; L-Phe, L-phenylalanine; LTBL, leukoencephalopathy with thalamus and brain stem involvement and lactate elevation; MELAS, mitochondrial myopathy, encephalopathy, lactic acidosis and stroke-like episodes; MERRF, myoclonic epilepsy with ragged red fibers; mitaaRSs, mitochondrial aminoacyl-tRNA synthetases; mitGlyRS, mitochondrial glycyl-tRNA synthetase; mitTyrRS, mitochondrial tyrosyl-tRNA synthetase; RC, respiratory chain; WT, wild-type*

© 2019 International Union of Biochemistry and Molecular Biology

Volume 71, Number 8, August 2019, Pages 1141–1149

**Address correspondence to: Rajat Banerjee, Department of Biotechnology and Dr. B. C. Guha Centre for Genetic Engineering and Biotechnology, University of Calcutta, 35, Ballygunge Circular Road, Kolkata 700019, India.*
Email: rbbcgc@gmail.com

Received 26 March 2019; Accepted 6 June 2019
DOI 10.1002/iub.2114
Published online 26 June 2019 in Wiley Online Library (wileyonlinelibrary.com)

vulnerable tissue is mostly associated with a particular mitaaRS (10, 11). Each of the 19 mitaaRSs is reported to have disease correlations and mutations in 17 out of 19 mitaaRSs (except mitGlyRS and mitTyrRS) encoding genes are found to be associated with damages in the central nervous system (12). For example, mutations in the mitochondrial aspartyl-tRNA synthetase gene (DARS2) have been found to be linked with leukoencephalopathy with brain stem and spinal cord involvement and lactate elevation (LBSL, MIM 611105), while mutations in the mitochondrial arginyl-tRNA synthetase gene (RARS2) lead to pontocerebellar atrophy type 6 (MIM 611523), and mutations in mitochondrial glutamyl-tRNA synthetase (EARS2) have been linked to leukoencephalopathy with thalamus and brain stem involvement and lactate elevation (LTBL, MIM 614924) (10, 11).

To date at least 21 pathogenic variants have been reported for *Hs*mitPheRS that were found to be associated with disease conditions with moderate to severe symptoms. The clinical phenotypic expression of the pathogenic variants of the FARS2 gene show pleiotropic effects, from spastic paraplegia to infantile Alpers encephalopathy (13–24). The effects of some of these mutations on enzyme function have been investigated. Initially three mutations (Y144C, I329T, and D391V) have been reported associated with Alpers encephalopathy with severe early-onset clinical symptoms and death in infancy. Studies of these mutants have reported to effect the enzymatic activity with possible indications of perturbation in enzyme stability (13, 14). We have now built on these earlier studies using biophysical approaches to understand the effect of these mutations on folding and stability of the *Hs*mitPheRS. Our findings revealed that the Alpers encephalopathy associated-mutations have a strong effect on the solubility of the enzyme in vitro, with significant implications for loss of function in vivo.

MATERIALS AND METHODS

Expression and purification of the pathogenic mutants of HsmitPheRS

pET21c plasmid with *Hs*mitPheRS (FARS2) gene containing Y144C, I329T, and D391V single mutations were transformed separately in *Escherichia coli* strain BL21 (DE3). Bacterial colonies were transferred and grown into Luria-Bertani (LB) media containing 100 μg/mL of Ampicillin from transformed plates for each plasmid DNA and grown overnight at 37°C. Fresh LB media containing Ampicillin were inoculated with the culture and grown at 37°C until $OD_{595\ nm}$ reaches to ~0.6. 10 mL of this culture were added to 1 L of Ampicillin-enriched autoinduction media and grown at 25°C overnight (25). The cells were harvested by centrifugation at 5,000 rpm for 10 min and further processed to purify the protein as was mentioned previously (26).

Fluorescence spectroscopy

All the fluorescence measurements were carried out in Hitachi F-7000 spectrofluorometer at least three times. Tryptophan was selectively excited at 295 nm and the emission was recorded from 310 to 450 nm. Both excitation and emission slit widths were set at 5 nm for all the measurements. The emission maxima (λ_{max}) values were determined by taking the first derivative of the individual emission spectra.

Acid denaturation

Acid denaturation of *Hs*mitPheRS was studied as a function of pH from pH 1.0 to pH 8.0 at a 0.5 interval using 50 mM buffers (KCl-HCl [pH 1.0–1.5], Gly-HCl [pH 2.0–3.5], sodium acetate [pH 4.0–5.5], and sodium phosphate [pH 6.0–8.0]). All reagents used for buffer preparation were of analytical (AR) grade. The buffers were filtered through 0.22 μm membrane filter, and stored at −20°C and thawed to room temperature before use. Protein samples were added individually at different pH values to a final concentration of 2 μM and incubated at room temperature for 18–24 hr to ensure that thermodynamic equilibrium has been reached.

ANS binding assay

8-Anilino-1-naphthalenesulfonic acid (ANS) is a fluorescent molecular probe that hardly fluoresces in aqueous environment but fluoresces only when it binds to hydrophobic regions of proteins. A stock solution of ANS was prepared in methanol and the concentration was determined using an extinction coefficient of 5,000 M^{-1} cm^{-1} at 350 nm. Protein samples (2 μM) were incubated with 25-fold molar excess of ANS for 30 min in the dark at room temperature. The ANS fluorescence was then measured by setting the excitation wavelength at 420 nm to avoid the inner filter effect and emission spectra were recorded from 450 nm to 550 nm. Fluorescence intensities at 482 nm were recorded and plotted as a function of pH.

Turbidity assay

Turbidity of the ligand free protein samples (2 μM) were measured in 50 mM Tris–HCl (pH 8.0), 5 mM $MgCl_2$, 150 mM KCl without any substrates. Turbidity of the protein samples (2 μM) were also measured in presence of 2 mM of L-phenylalanine (L-Phe) and 2 mM of L-Phe with 2 mM of ATP. The turbidity was measured at 400 nm at 37°C over time in a Shimadzu UV-2401PC spectrophotometer equipped with a Peltier temperature controller. All the measurements were done in triplicates and the average was plotted against time.

Dynamic light scattering (DLS)

Protein samples (4 μM) in 50 mM Tris–HCl (pH 8.0), 5 mM $MgCl_2$, 150 mM KCl were filtered through 0.22 μm filter device from Millipore and transferred to disposable cuvettes and the hydrodynamic diameters were determined in Malvern Zetasizer™ NanoS light scattering instrument. The protein samples were subjected to a temperature gradient from 25°C to 40°C and the change in the hydrodynamic diameters was monitored by DLS. The effect of substrates were studied in presence of 2 mM of L-Phe and 2 mM ATP by setting the temperature at 37°C and the change in particle size was determined by DLS for 1 hr.

The thermoflour experiment

The assay was performed using 96-well thin-wall PCR plates (Applied Biosystems, US). The total reaction volume was 30 μL

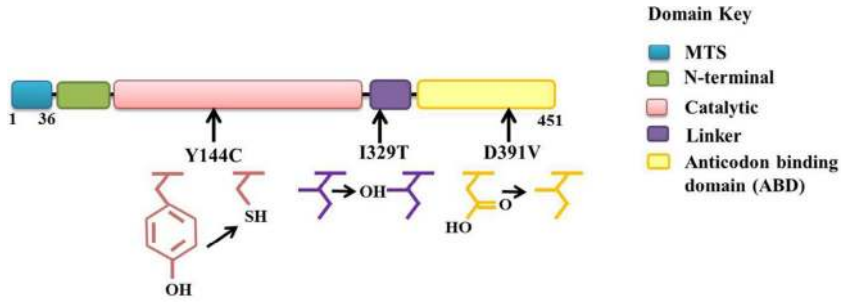

FIG 1 *Location and chemical nature of the amino acid substitutions of the Alpers encephalopathy associated mutants within the functional domains of* Hs*mitPheRS*

and the plate was kept on ice while adding the samples. The final protein concentration was kept at 4 μM. 5000X SYPRO Orange stock solution was diluted 100-fold in buffer (50 mM Tris pH 8.0, 5 mM $MgCl_2$, 50 mM NaCl) to get a 10-fold working solution. Three microliters of the 10-fold SYPRO Orange working solution was added to each reaction. The plates were sealed with optical adhesive covers (Applied Biosystems) and centrifuged at 4000 rev/min for 2 min. The plate was then heated from 25 to 80°C in the StepOne real-time PCR system from Applied Biosystems for the thermoflour experiment. Variation in fluorescence in the wells was monitored using excitation and emission wavelength of 492 and 516 nm, respectively. The inflection point of the fluorescence intensity versus temperature plot was considered to be the transition mid-point (*Tm*) (27).

RESULTS

Mutations of HsmitPheRS in sequence and structural context

Mutations of the conserved residues are usually believed to be detrimental to enzyme architecture that may affect their function. Multiple sequence alignment of mitPheRS showed that all three amino acid residues mutated in Alpers encephalopathy patients, Tyr144, Ile329, and Asp391 are highly conserved among all the mitPheRS(14) that may lead to structural and/or functional perturbation in the enzyme. The amino acid substitutions have been shown to affect the substrate affinity of the enzyme. While I329T affects ATP binding, D391V affects the L-Phe binding and Y144C affects $tRNA^{Phe}$ binding of *Hs*mitPheRS. From a structural perspective it is predicted that the Ile to Thr mutation at 329 position leads to widening of the ATP-binding site whereas Y144C and D391V variants are believed to affect the conformational flexibility of the enzyme because Tyr144 is located on the interface of the anticodon stem-binding domain and Asp391 is located on the contact surface of the aminoacylation and the anticodon binding domains(14) (Figure 1). The functional perturbations of these amino acid substitutions led us to investigate the structural implications on the enzyme, if any, under different conditions using biophysical approaches.

Formation of stable molten-globule-like structure at acidic pH

To understand the effect of these amino acid substitutions on protein stability over a range of pH, denaturation studies were

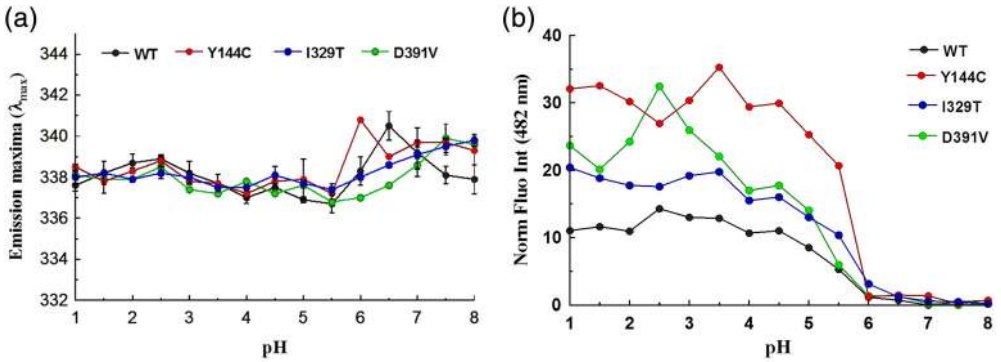

FIG 2 *Change in conformation of* Hs*mitPheRS as a function of pH. (a) pH-induced changes in tryptophan emission maxima of* Hs*mitPheRS. Tryptophan emission maxima were obtained by taking the first derivative of the tryptophan emission spectra in Hitachi F-7000 spectrofluorometer. All the data were recorded three times and standard deviations were calculated. (b) ANS binding as a function of pH. Fluorescence intensities at 482 nm were recorded in Hitachi F-7000 spectrofluorometer and plotted as a function of pH. The data are average of three measurements*

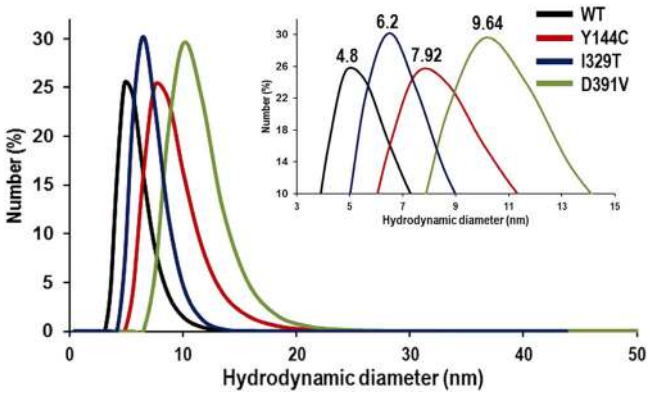

FIG 3

Comparative size of the WT and the pathogenic variants of HsmitPheRS. *Particle hydrodynamic diameter (d_H) distribution by number (%) as measured by DLS in Malvern Zetasizer™ NanoS light scattering instrument. Protein concentration was kept 4 μM in 50 mM Tris–HCl (pH 8.0), 5 mM $MgCl_2$, 150 mM KCl buffer*

done using buffer ranging from pH 1.0 to 8.0. Measurement of tryptophan emission maxima change and ANS binding as a function of pH showed that the WT *Hs*mitPheRS is remarkably stable at lower pH. The pathogenic variants also showed comparable stability at low pH; however, at physiological pH (∼pH 8.0) the tryptophan emission maxima showed a red-shift of ∼2 nm compared to the WT indicating that the tryptophans are more exposed in the mutants with respect to the native conformation at physiological pH (Figure 2a). ANS fluorescence indicated that WT as well as the pathogenic variants form a molten-globule-like structure at low pH range (pH 1.0–pH 6.0) and the fluorescence leveled off above pH 6.0. Notably, the ANS binding at low pH is much higher in the case of the pathogenic variants compared to the WT (Figure 2b).

The pathogenic variants affect the enzyme architecture

Particle size distribution of WT and the pathogenic variants were determined by DLS to understand whether there is any

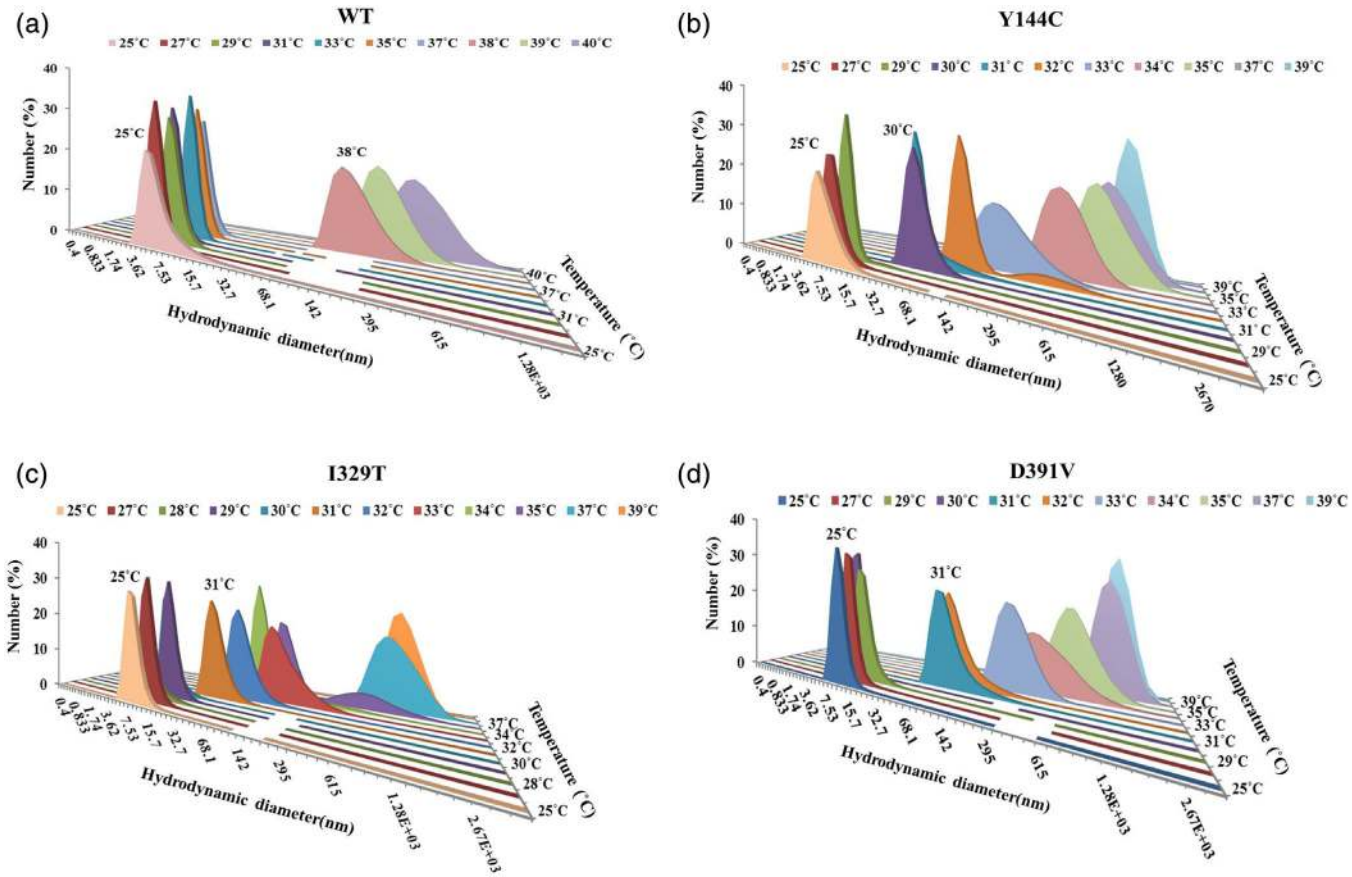

FIG 4

Determination of the starting temperature of aggregation of WT and the pathogenic variants by DLS. (a) Particle hydrodynamic diameter distribution by number (%) of WT as measured by DLS with increasing temperature. (b) Particle hydrodynamic diameter distribution by number (%) of Y144C as measured by DLS with increasing temperature. (c) Particle hydrodynamic diameter distribution by number (%) of I329T as measured by DLS with increasing temperature. (d) Particle hydrodynamic diameter distribution by number (%) of D391V as measured by DLS with increasing temperature

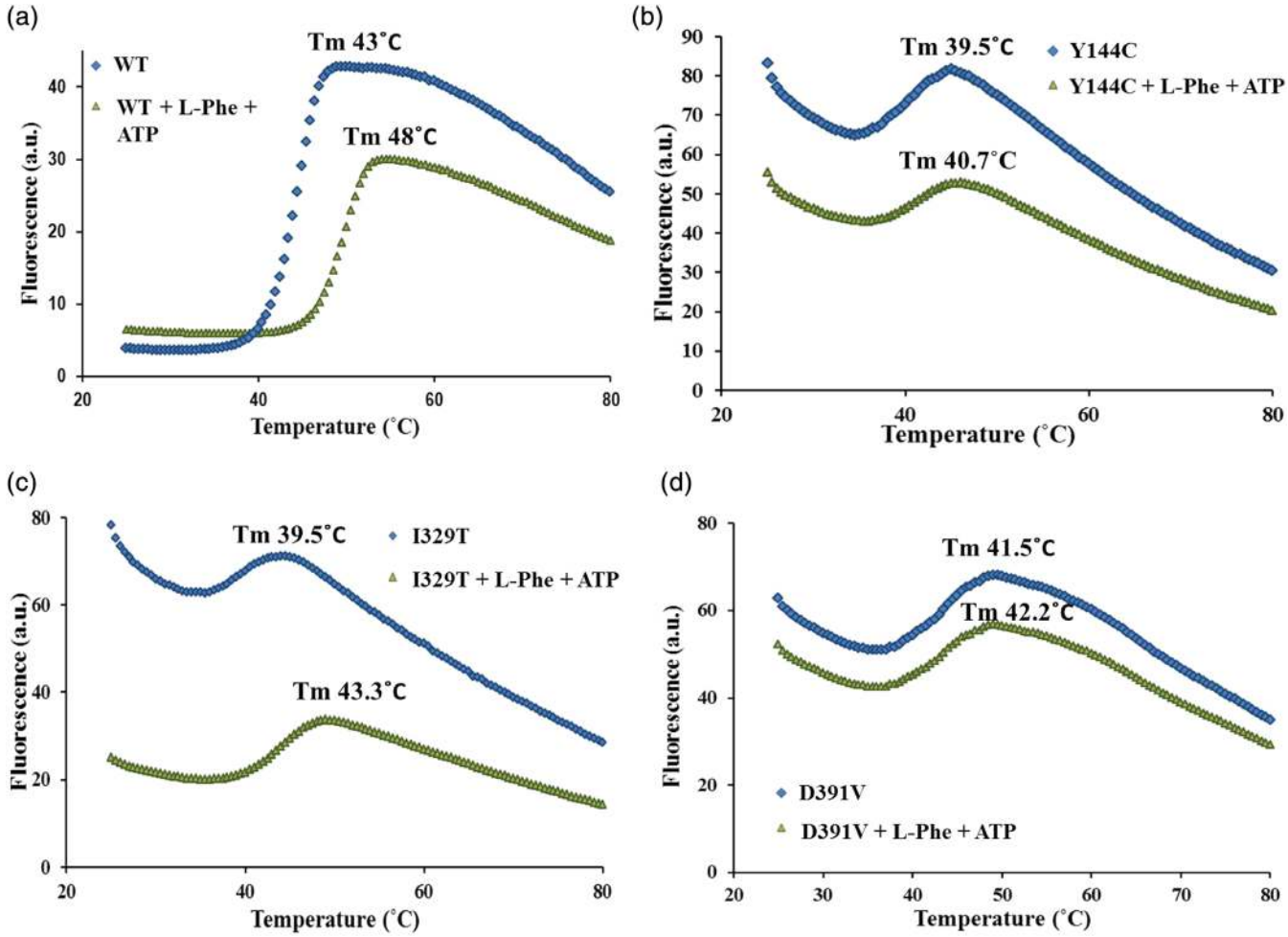

FIG 5

Differential thermal stability of the WT Hs*mitPheRS and the pathogenic variants. (a) Temperature-dependent binding of SYPRO Orange to WT, in absence and in presence of L-Phe and ATP as was determined by thermoflour assay. (b) Temperature-dependent binding of SYPRO Orange to Y144C, in absence and in presence of L-Phe and ATP as was determined by thermoflour assay. (c) Temperature-dependent binding of SYPRO Orange to I329T, in absence and in presence of L-Phe and ATP as was determined by thermoflour assay. (d) Temperature-dependent binding of SYPRO Orange to D391V, in absence and in presence of L-Phe and ATP as was determined by thermoflour assay*

perturbation in enzyme architecture in case of the variants at physiological pH. The results indicated that the hydrodynamic diameter (d_H) of the WT protein is 4.8 ± 0.7 nm, whereas the size of all three pathogenic mutants (Y144C, 7.9 ± 0.6 nm; I329T, 6.2 ± 0.5 nm; D391V, 9.64 ± 0.8 nm) (Figure 3) increased significantly from the WT indicating that the pathogenic mutations may lead to a conformational expansion of *Hs*mitPheRS in solution affecting the enzyme's native architecture.

Thermal stability of the mutants decreased significantly

To understand whether there are any differences in stability between WT and the pathogenic variants of *Hs*mitPheRS, they were subjected to thermal denaturation. Two approaches were used to assess the changes in thermal stability, the propensity to aggregate with increasing temperature as recorded by DLS and exposure of the hydrophobic patches to solvent upon unfolding with increasing temperature as recorded by real time PCR. Thermal stability of the pathogenic variants was compared with WT by heating them gradually from 25 to 40°C and monitoring the aggregation by DLS. The temperature at which the WT *Hs*mitPheRS started aggregating is 38 ± 1°C. In case of Y144C the aggregation started at 30 ± 1°C, while I329T and D391V, both the mutants started aggregating at 31 ± 1°C (Figure 4a–d). These data indicate that the stability of the pathogenic variants is highly compromised compared to the WT HsmitPheRS.

For the thermoflour experiments, binding of a hydrophobic fluorescent dye, SYPRO Orange, was monitored while increasing the temperature gradually from 25 to 80°C. SYPRO Orange undergoes a significant increase in quantum yield upon binding to hydrophobic regions of proteins that become exposed upon protein denaturation. The transition mid-point temperature (T_m) was determined from the increase of fluorescence intensity

TABLE 1 *Increase in the melting temperature (ΔT_m) of HsmitPheRS in presence of L-Phe and ATP*

Hs*mitPheRS*	ΔT_m (°C) (Phe-AMP)
WT	5
Y144C	1.2
I329T	3.8
D391V	0.7

of SYPRO Orange upon binding to hydrophobic patches of protein. The stabilizing effect on thermal stability of the phenyladenylate (Phe-AMP) complex, which binds to the active site of the enzyme, was checked for the WT as well as the mutants. In the case of WT, the transition mid-point temperature was 43°C without any substrate addition. Phe-AMP exerted a strong stabilizing effect, increasing the T_m to 48°C (ΔT_m = + 5°C). The T_m of the mutants decreased ~1.5–3°C from the WT (Y144C, T_m– 39.5°C; I329T, T_m– 39.5°C; D391V, T_m– 41.5°C); however, the stabilizing effect of Phe-AMP was less pronounced for mutants compared to WT HsmitPheRS (Figure 5a–d; Table 1). While Phe-AMP is able to somewhat stabilize the I329T variant, the other two mutants, Y144C and D391V, are only marginally stable in the presence of Phe-AMP. Very high fluorescence values even at a lower temperature in the case of the pathogenic variants compared to WT is indicative of the fact that all three amino acid substitutions in *Hs*mitPheRS have reduced stability and may lead to a conformational opening of the enzyme making them prone to aggregation. These findings are consistent with the DLS data that displayed a larger particle size of the variants compared to WT *Hs*mitPheRS. The severe impact of these amino acid

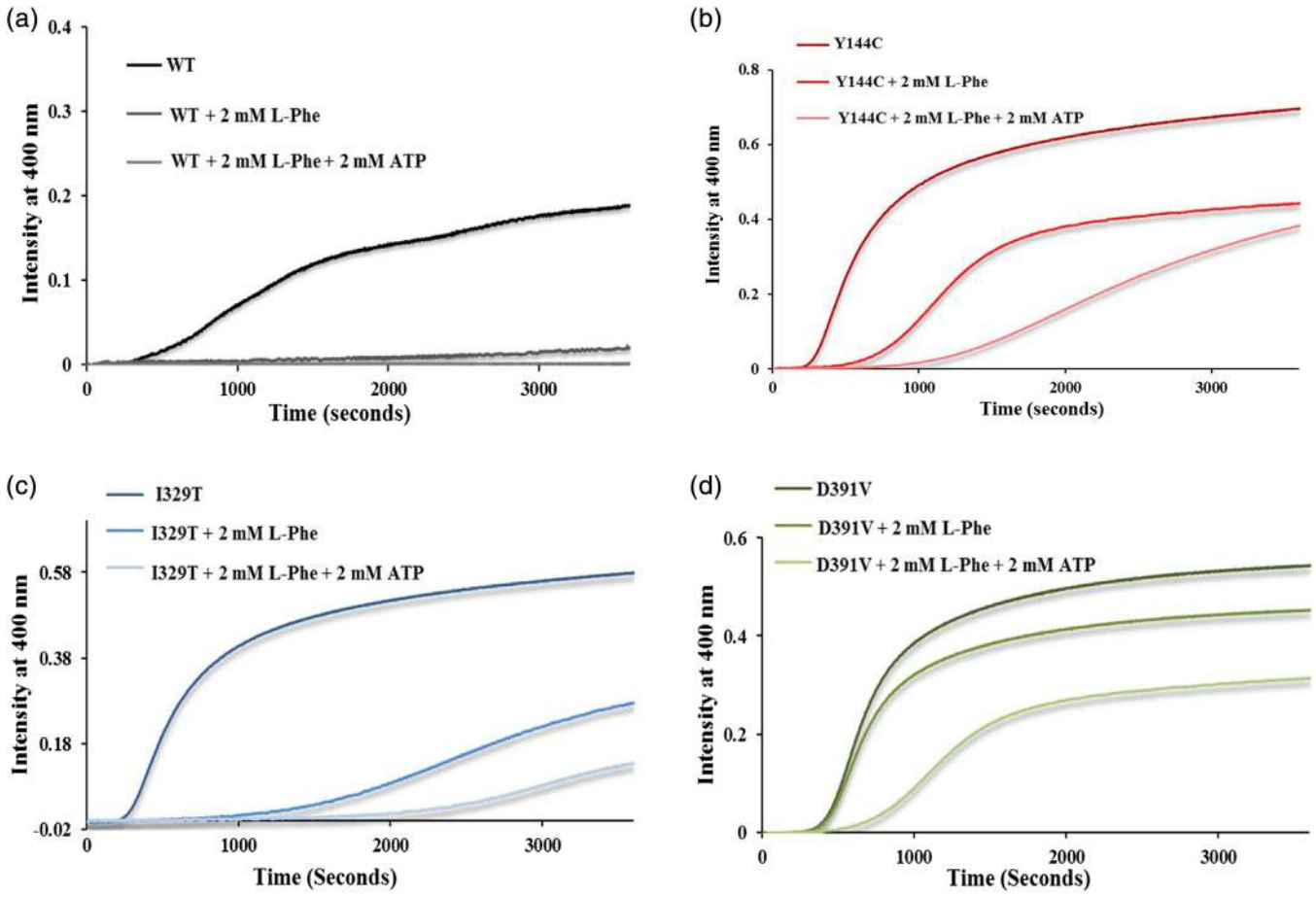

FIG 6 *Turbidity assay of the WT and the pathogenic variants of* Hs*mitPheRS. (a) Turbidity assay of the WT* Hs*mitPheRS in ligand free condition, in presence of L-Phe, and in presence of L-Phe and ATP. (b) Turbidity assay of the Y144C in ligand free condition, in presence of L-Phe, and in presence of L-Phe and ATP. (c) Turbidity assay of the I329T variant in ligand free condition, in presence of L-Phe, and in presence of L-Phe and ATP. (d) Turbidity assay of the D391V variant in ligand free condition, in presence of L-Phe, and in presence of L-Phe and ATP*

substitutions on protein stability raises the question of how these mutations impact stability of *Hs*mitPheRS in the cellular milieu at body temperature.

DISCUSSION

Mitochondrial proteins that are synthesized in the cytosol have to undergo either a partial or complete unfolding driven by the protein import machineries or the mitochondrial membrane potential to facilitate the transportation process across the mitochondrial membrane (28). It has previously been established that *Hs*mitPheRS undergoes a low pH-induced partial unfolding that may actually facilitate the transport process due to the generation of a local pH gradient across the mitochondrial membrane (26). The pathogenic variants studied here were additionally found to form a molten globule-like structure at lower pH, and showed increased ANS fluorescence at lower pH compared to WT *Hs*mitPheRS, indicating that the hydrophobic patches are much more exposed to solvents in the variants than in WT.

Determination of the particle size of the pathogenic variants at physiological pH by DLS showed increase in diameter compared to the WT enzyme giving rise to a possibility that there may be a conformational perturbation of the enzyme due to these amino acid variations. This structural perturbation may also compromise the stability of the mutants as specified from the thermal denaturation data. In the case of GlyRS, it has been established using hydrogen-deuterium exchange that five spatially dispersed mutations associated with Charcot–Marie–Tooth (CMT) disease leads to a similar conformational opening of the in-solution conformation of the enzyme (29). Accumulation of aberrant misfolded proteins as amyloidogenic aggregates are found to be the common hallmark of many neurological diseases, like Parkinson's disease, Alzheimer's disease, amyotrophic lateral sclerosis, and so forth. Several disease-associated mutations in specific proteins such as α-synuclein, TDP-43, tau lead to protein misfolding and aggregate formation leading to cellular dysfunction and eventually brain damage (30, 31). Protein misfolding leading to decreased solubility may also affect the availability of the functional protein to sustain its normal activity (32). Biophysical approaches to understand the effect of these mutations on enzyme properties have proven that they alter the stability and solubility of the enzyme. The aminoacylation-intermediate complex has been shown to have a stabilizing effect on structure(32–34) and is also used frequently for structural studies to stabilize the catalytic region (35, 36). The aggregation kinetics data of the mutants at 37°C in the presence of L-Phe and ATP by both static light scattering (SLS) and DLS experiments (Figures 6a–d and 7) suggested that binding of the Phe-AMP complex does not have as pronounced an effect on stability in the case of the pathogenic variants as was seen for the WT *Hs*mitPheRS. The stabilizing effect of the Phe-AMP complex was nominal in the case of the pathogenic variants, especially Y144C and D391V. The deleterious effect of the

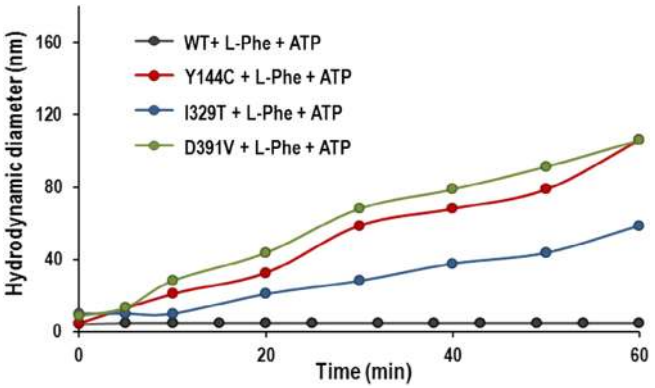

FIG 7 *Determination of the particle size of the WT and the pathogenic variants of* Hs*mitPheRS in presence of substrates by DLS as a function of time. Particle hydrodynamic diameter distribution by number (%) as measured by DLS in presence of L-Phe and ATP at 37° C as a function of time*

mutants on thermal stability and solubility of the enzyme at physiological pH may have a strong impact on the amount of functional *Hs*mitPheRS available in mitochondria under pathological conditions. These observations extend the need to explore the in-solution structure and cellular availability of the enzyme under disease conditions. Based on the patient history and reported enzymatic activities of pathogenic missense mutations of *Hs*mitPheRS it is hard to draw any genotype–phenotype correlation. Recent studies on the effect of some of these variants on structure and function of *Hs*mitPheRS impede any direct correlation as many of the less conserved residues showed severe impact on enzyme activity and vice versa (37). In vitro studies of enzymatic activities are also not always corroborative with the clinical phenotypes indicating that there is a potential difference in in vitro and in vivo enzyme function. Earlier three patients with homozygous Y144C mutations have been reported and two patients with compound heterozygous mutations (I329T and D391V) were reported of which all the patients died in their infancy (13, 14). Recently, 11 patients with Y144C homozygous mutations and a patient with compound heterozygous mutations (Y144C and V177D) have been reported. All of the 12 patients showed severe clinical phenotypes with reduced life expectancy, the patient with the compound heterozygous mutations being the most severe among the patients reported until now with FARS2 mutations (24). Biophysical characterization of the pathogenic variants in this study has shown consistently compromised conformational stability of *Hs*mitPheRS mutants in addition to changes in their residual activities that may contribute to the severe clinical phenotypes in the corresponding patients. Compromised enzymatic activity and stability may exert accumulative depletion on the housekeeping function of *Hs*mitPheRS in mitochondria that may in turn lead to insufficient synthesis of Phe-tRNA^{Phe} to sustain normal mitochondrial translation. However, it is still premtaure to conclude a direct correlation between pathogenic variants and their in vitro aminoacylation

activities and stability, as there remain many unknown factors still to consider (38). To this end, studies of the HmitPheRS and its pathogenic mutants may be developed as model to decipher the mechanistic pathway of mutant mitochondrial aaRSs-related diseases with the help of numerous crystal structures of free-and tRNA-bound proteins including several pathogenic mutants (37, 39, 40).

ACKNOWLEDGMENTS

The present study was supported by a grant from the DST-SERB (sanction order no. EMR/2016/002247) to RB and the National Science Foundation (MCB 1715840) to MI. SC is supported by a fellowship from the University Grant Commission (UGC), Government of India. The authors thank Dr. Alok Kumar Sil, University of Calcutta for allowing to use the StepOne real-time PCR system from Applied Biosystems in his laboratory. The authors thank Mr. Dipak C. Konar (Bose Institute) for technical support.

AUTHOR CONTRIBUTIONS

S.C., M.I., and R.B. designed the experiments and analyzed the data. S.C. performed the experiments. S.C., M.I., and R.B. wrote the manuscript.

CONFLICT OF INTEREST

The authors declare no potential conflict of interest.

REFERENCES

[1] Montoya J, López-Gallardo E, Díez-Sánchez C, López-Pérez MJ, Ruiz-Pesini E. 20 years of human mtDNA pathologic point mutations: Carefully reading the pathogenicity criteria. Biochim Biophys Acta. 2009;1787:476–483.

[2] Khan NA, Govindaraj P, Meena AK, Thangaraj K. Mitochondrial disorders: Challenges in diagnosis & treatment. Indian J Med Res. 2015;141:13–26.

[3] Craven L, Alston CL, Taylor RW, Turnbull DM. Recent advances in mitochondrial disease. Annu Rev Genomics Hum Genet. 2017;18:257–275.

[4] Tuppen HA, Blakely EL, Turnbull DM, Taylor RW. Mitochondrial DNA mutations and human disease. Biochim Biophys Acta. 2010;1797:113–128.

[5] Pütz J, Dupuis B, Sissler M, Florentz C. Mamit-tRNA, a database of mammalian mitochondrial tRNA primary and secondary structures. RNA. 2007;13:1184–1190.

[6] Roos S, Darin N, Kollberg G, et al. A novel mitochondrial tRNA Arg mutation resulting in an anticodon swap in a patient with mitochondrial encephalomyopathy. Eur J Hum Genet. 2013;21:571–573.

[7] Lu Y, Zhao D, Yao S, et al. Mitochondrial tRNA genes are hotspots for mutations in a cohort of patients with exercise intolerance and mitochondrial myopathy. J Neurol Sci. 2017;379:137–143.

[8] Heidari MM, Keshmirshekan A, Bidakhavidi M, et al. A novel heteroplasmic mutation in mitochondrial tRNA(Arg) gene associated with non-dystrophic myotonias. Acta Neurol Belg. 2018. https://doi.org.10.1007/s13760-018-1042-5

[9] Sissler M, González-Serrano LE, Westhof E. Recent advances in mitochondrial Aminoacyl-tRNA Synthetases and disease. Trends Mol Med. 2017;23:693–708.

[10] Diodato D, Ghezzi D, Tiranti V. The mitochondrial Aminoacyl tRNA Synthetases: Genes and syndromes. Int J Cell Biol. 2014;2014:787956.

[11] Yao P, Fox PL. Aminoacyl-tRNA synthetases in medicine and disease. EMBO Mol Med. 2013;5:332–343.

[12] Moulinier L, Ripp R, Castillo G, Poch O, Sissler M. MiSynPat: An integrated knowledge base linking clinical, genetic, and structural data for disease-causing mutations in human mitochondrial aminoacyl-tRNA synthetases. Hum Mutat. 2017;38:1316–1324.

[13] Shamseldin HE, Alshammari M, Al-Sheddi T, et al. Genomic analysis of mitochondrial diseases in a consanguineous population reveals novel candidate disease genes. J Med Genet. 2012;49:234–241.

[14] Elo JM, Yadavalli SS, Euro L, et al. Mitochondrial phenylalanyl-tRNA synthetase mutations underlie fatal infantile Alpers encephalopathy. Hum Mol Genet. 2012;21:4521–4529.

[15] Almalki A, Alston CL, Parker A, et al. Mutation of the human mitochondrial phenylalanine-tRNA synthetase causes infantile-onset epilepsy and cytochrome c oxidase deficiency. Biochim Biophys Acta. 2014;1842:56–64.

[16] Vernon HJ, McClellan R, Batista DA, Naidu S. Mutations in FARS2 and non-fatal mitochondrial dysfunction in two siblings. Am J Med Genet A. 2015;167:1147–1151.

[17] Yang Y, Liu W, Fang Z, et al. A newly identified missense mutation in FARS2 causes autosomal-recessive spastic paraplegia. Hum Mutat. 2016;37:165–169.

[18] Wang J, Li JL, Schmitt ES, Peacock S, Zhang VW, Wong L-J. Novel pathogenic variants in the mitochondrial aminoacyl TRNA synthetases genes. Mol Genet Metab. 2015;114:352–353.

[19] Raviglione F, Conte G, Ghezzi D, et al. Clinical findings in a patient with FARS2 mutations and early-infantile-encephalopathy with epilepsy. Am J Med Genet A. 2016;170:3004–3007.

[20] Walker MA, Mohler KP, Hopkins KW, et al. Novel compound heterozygous mutations expand the recognized phenotypes of FARS2-linked disease. J Child Neurol. 2016;31:1127–1137.

[21] Cho JS, Kim SH, Kim HY, et al. FARS2 mutation and epilepsy: Possible link with early-onset epileptic encephalopathy. Epilepsy Res. 2017;129:118–124.

[22] Vantroys E, Larson A, Friederich M, et al. New insights into the phenotype of FARS2 deficiency. Mol Genet Metab. 2017;122:172–181.

[23] Sahai SK, Steiner RE, Au MG, et al. FARS2 mutations presenting with pure spastic paraplegia and lesions of the dentate nuclei. Ann Clin Transl Neurol. 2018;5:1128–1133.

[24] Almannai M, Wang J, Dai H, et al. FARS2 deficiency; new cases, review of clinical, biochemical, and molecular spectra, and variants interpretation based on structural, functional, and evolutionary significance. Mol Genet Metab. 2018;125:281–291.

[25] Tyler RC, Sreenath HK, Singh S, et al. Auto-induction medium for the production of [U-15N]- and [U-13C, U-15N]-labeled proteins for NMR screening and structure determination. Protein Expr Purif. 2005;40:268–278.

[26] Banerjee R, Reynolds NM, Yadavalli SS, et al. Mitochondrial aminoacyl-tRNA synthetase single-nucleotide polymorphisms that lead to defects in refolding but not aminoacylation. J Mol Biol. 2011;410:280–293.

[27] Reinhard L, Mayerhofer H, Geerlof A, Mueller-Dieckmann J, Weiss MS. Optimization of protein buffer cocktails using Thermofluor. Acta Crystallogr Sect F Struct Biol Cryst Commun. 2013;69:209–214.

[28] Schwartz MP, Huang S, Matouschek A. The structure of precursor proteins during import into mitochondria. J Biol Chem. 1999;274:12759–12764.

[29] He W, Zhang HM, Chong YE, Guo M, Marshall AG, Yang XL. Dispersed disease-causing neomorphic mutations on a single protein promote the same localized conformational opening. Proc Natl Acad Sci U S A. 2011;108:12307–12312.

[30] Lázaro DF, Rodrigues EF, Langohr R, et al. Systematic comparison of the effects of alpha-synuclein mutations on its oligomerization and aggregation. PLoS Genet. 2014;10:e1004741.

[31] Janssens J, Van Broeckhoven C. Pathological mechanisms underlying TDP-43 driven neurodegeneration in FTLD-ALS spectrum disorders. Hum Mol Genet. 2013;22:R77–R87.

[32] Sauter C, Lorber B, Gaudry A, et al. Neurodegenerative disease-associated mutants of a human mitochondrial aminoacyl-tRNA synthetase present individual molecular signatures. Sci Rep. 2015;5:17332.

[33] Messmer M, Blais SP, Balg C, et al. Peculiar inhibition of human mitochondrial aspartyl-tRNA synthetase by adenylate analogs. Biochimie. 2009;91:596–603.
[34] Neuenfeldt A, Lorber B, Ennifar E, et al. Thermodynamic properties distinguish human mitochondrial aspartyl-tRNA synthetase from bacterial homolog with same 3D architecture. Nucleic Acids Res. 2013;41:2698–2708.
[35] Giegé R, Touzé E, Lorber B, Téobald-Dietrich A, Sauter C. Crystallogenesis trends of free and liganded aminoacyl-tRNA synthetases. Cryst Growth Des. 2008;8:4297–4306.
[36] Bonnefond L, Schellenberger P, Basquin J, et al. Exploiting protein engineering and crystal polymorphism for successful X-ray structure determination. Cryst Growth Des. 2011;11:4334–4343.
[37] Kartvelishvili E, Tworowski D, Vernon H, et al. Kinetic and structural changes in HsmtPheRS, induced by pathogenic mutations in human FARS2. Protein Sci. 2017;26(8):1505–1516.
[38] González-Serrano LE, Chihade JW, Sissler M. When a common biological role does not imply common disease outcomes: Disparate pathology linked to human mitochondrial aminoacyl-tRNA synthetases. J Biol Chem. 2019;294:5309–5320.
[39] Klipcan L, Levin I, Kessler N, Moor N, Finarov I, Safro M. The tRNA-induced conformational activation of human mitochondrial phenylalanyl-tRNA synthetase. Structure. 2008;16:1095–1104.
[40] Klipcan L, Moor N, Finarov I, Kessler N, Sukhanova M, Safro MG. Crystal structure of human mitochondrial PheRS complexed with tRNA(Phe) in the active "open" state. J Mol Biol. 2012;415:527–537.